

Measurement of the Spin-Orbit Alignment in the Exoplanetary System HD 189733¹

Joshua N. Winn², John Asher Johnson³, Geoffrey W. Marcy³, R. Paul Butler⁴,
Steven S. Vogt⁵, Gregory W. Henry⁶, Anna Roussanova², Matthew J. Holman⁷,
Keigo Enya⁸, Norio Narita⁹, Yasushi Suto⁹, Edwin L. Turner¹⁰

ABSTRACT

We present spectroscopy of a transit of the exoplanet HD 189733b. By modeling the Rossiter-McLaughlin effect (the anomalous Doppler shift due to the partial eclipse of the rotating stellar surface), we find the angle between the sky projections of the stellar spin axis and orbit normal to be $\lambda = -1.4 \pm 1.1$. This is the third case of a “hot Jupiter” for which λ has been measured. In all three cases λ is small, ruling out random orientations with 99.96% confidence, and suggesting that the inward migration of hot Jupiters generally preserves spin-orbit alignment.

Subject headings: planetary systems — planetary systems: formation — stars: individual (HD 189733) — stars: rotation

¹Data presented herein were obtained at the W.M. Keck Observatory, which is operated as a scientific partnership among the California Institute of Technology, the University of California, and the National Aeronautics and Space Administration, and was made possible by the generous financial support of the W. M. Keck Foundation.

²Department of Physics, and Kavli Institute for Astrophysics and Space Research, Massachusetts Institute of Technology, Cambridge, MA 02139, USA

³Department of Astronomy, University of California, Mail Code 3411, Berkeley, CA 94720, USA

⁴Department of Terrestrial Magnetism, Carnegie Institution of Washington, 5241 Broad Branch Road NW, Washington D.C. USA 20015-1305

⁵UCO/Lick Observatory, University of California at Santa Cruz, Santa Cruz CA USA 95064

⁶Center of Excellence in Information Systems, Tennessee State University, 3500 John A. Merritt Blvd., Box 9501, Nashville, TN 37209, USA

⁷Harvard-Smithsonian Center for Astrophysics, 60 Garden Street, Cambridge, MA 02138, USA

⁸Institute of Space and Astronautical Science, Japan Aerospace Exploration Agency, 3-1-1, Yoshinodai, Sagami-hara, Kanagawa, 229-8510, Japan

⁹Department of Physics, The University of Tokyo, Tokyo 113-0033, Japan

¹⁰Princeton University Observatory, Peyton Hall, Princeton, NJ 08544, USA

1. Introduction

A primary reason to study planets of other stars is to learn how typical (or unusual) are the properties of the Solar system. For example, the nearly circular orbits of Solar system planets were once considered normal, but we now know that eccentric orbits of Jovian planets are common (see, e.g., Halbwachs, Mayor, & Udry 2005; or Fig. 3 of Marcy et al. 2005). Likewise, gas giants were once thought to inhabit only the far reaches of planetary systems, an assumption that was exploded by the discovery of “hot Jupiters” (Mayor & Queloz 1995, Butler et al. 1997). This inspired theoretical work on planetary migration mechanisms that can deliver Jovian planets to such tight orbits (as recently reviewed by Thommes & Lissauer 2005 and Papaloizou & Terquem 2006).

Another striking pattern in the Solar system is the close alignment between the planetary orbits and the Solar spin axis. The orbit normals of the 8 planets are within a few degrees of one another (Cox et al. 2000, p. 295), and the Earth’s orbit normal is only 7 degrees from the Solar spin axis (Beck & Giles 2005, and references therein). Presumably this alignment dates back 5 Gyr, when the Sun and planets condensed from a single spinning disk. Whether or not this degree of alignment is universal is unknown. For hot Jupiters in particular, one might wonder whether migration enforces or perturbs spin-orbit alignment.

For exoplanets, the angle between the stellar spin axis and planetary orbit normal (as projected on the sky) can be measured via the Rossiter-McLaughlin (RM) effect: the spectral distortion observed during a transit due to stellar rotation. The planet hides some of the velocity components that usually contribute to line broadening, resulting in an “anomalous Doppler shift” (for the theory, see Ohta et al. 2005, Giménez 2006, or Gaudi & Winn 2006).

Observations of the exoplanetary RM effect have been reported for HD 209458 (Bundy & Marcy 2000, Queloz et al. 2000, Winn et al. 2005, Wittenmyer et al. 2005) and HD 149026 (Wolf et al. 2006). Here we report observations of the RM effect for HD 189733. This system, discovered by Bouchy et al. (2005), consists of a K dwarf with a transiting Jovian planet ($M_P = 1.15 M_{\text{Jup}}$) in a 2.2 day orbit. Our observations are presented in § 2, our model in § 3, and our results in § 4, followed by a brief summary and discussion.

2. Observations

We observed the transit of UT 2006 August 21 with the Keck I 10m telescope and the High Resolution Echelle Spectrometer (HIRES; Vogt et al. 1994) following the usual protocols of the California-Carnegie planet search, as summarized here. We employed the red cross-disperser and placed the I₂ absorption cell into the light path to calibrate the

instrumental response and the wavelength scale. The slit width was $0''.85$ and the typical exposure time was 3 minutes, giving a resolution of 70,000 and a signal-to-noise ratio (SNR) of 300 pixel^{-1} . We obtained 70 spectra over 7.5 hr bracketing the predicted transit midpoint. To these were added 16 spectra that had been obtained by the California-Carnegie group at random orbital phases.

We determined the relative Doppler shifts with the algorithm of Butler et al. (1996). We estimated the measurement uncertainties based on the scatter in the solutions for each 2 \AA section of the spectrum. For the spectra obtained on 2006 Aug 21 the typical measurement error was 0.8 m s^{-1} , while for the other 16 spectra the error was $\approx 1.3 \text{ m s}^{-1}$. The data are given in Table 1 and plotted in Fig. 1, with enlarged error bars to account for the intrinsic velocity noise of the star (see § 3).

We also needed accurate photometry to pin down the planetary and stellar radii and the orbital inclination. We observed the transit of UT 2006 Jul 21 with KeplerCam on the 1.2m telescope at the Fred L. Whipple Observatory on Mt. Hopkins, Arizona. We used the SDSS z band filter and an exposure time of 30 seconds. After bias subtraction and flat-field division, we performed aperture photometry of HD 189733 and 14 comparison stars. The light curve of each comparison star was normalized to have unit median, and the mean of these normalized light curves was taken to be the comparison signal. The light curve of HD 189733 was divided by the comparison signal, and corrected for residual systematic effects by dividing out a linear function based on the out-of-transit data. The light curve is plotted in the top panel of Fig. 1.

3. The Model

We fitted the fluxes and radial velocities with a parameterized model based on a star and planet in a circular orbit about the center of mass.¹ To calculate the relative flux as a function of the projected separation of the planet and the star, we assumed the limb darkening law to be quadratic and employed the analytic formulas of Mandel & Agol (2002) to compute the integral of the intensity over the unobscured portion of the stellar disk. We fixed the limb-darkening coefficients at the values $u_1 = 0.320$, $u_2 = 0.267$, based on the calculations of Claret (2004).

To calculate the anomalous Doppler shift, we used the technique of Winn et al. (2005):

¹A circular orbit is a reasonable simplifying assumption because of the effects of tidal circularization (see, e.g., Rasio et al. 1996, Trilling et al. 2000, Dobbs-Dixon et al. 2004).

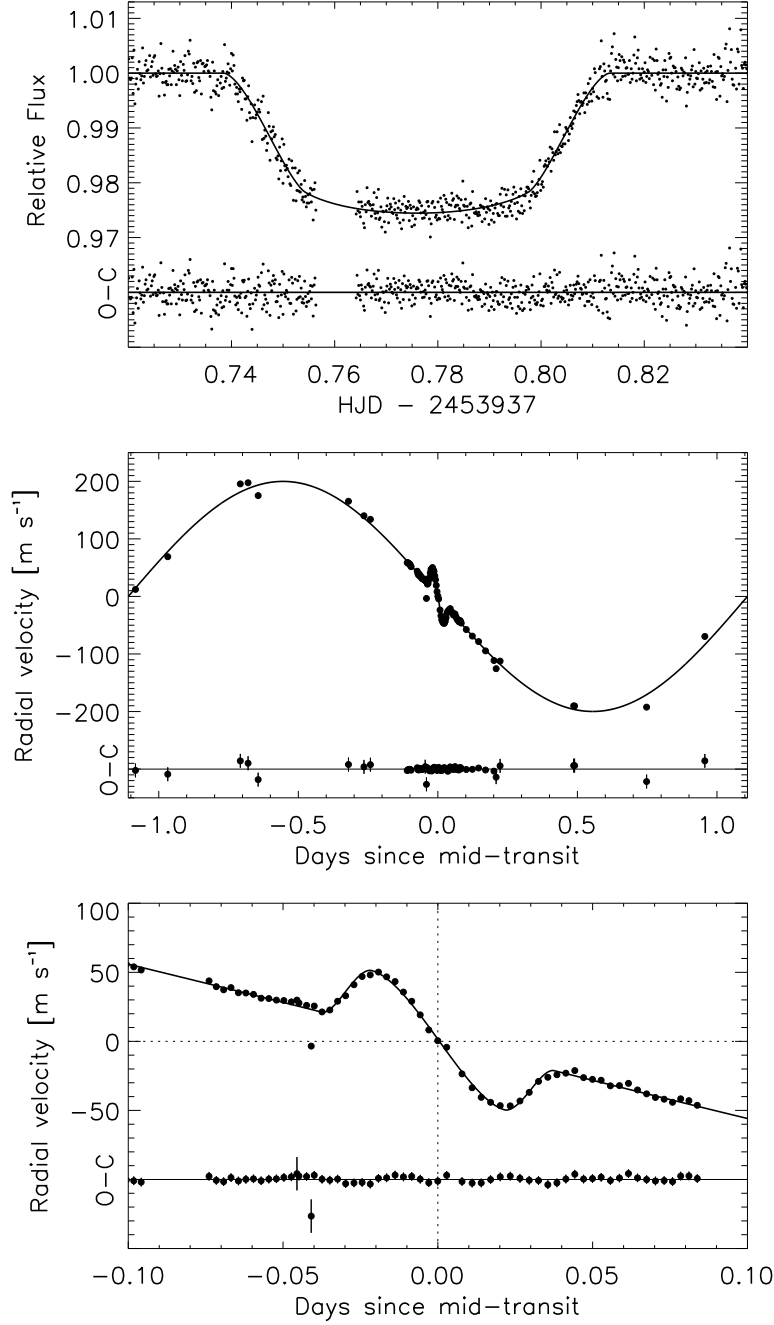


Fig. 1.— Photometry and spectroscopy of HD 189733. The top panel shows z band photometry during a transit, along with the best-fitting model (solid line). The middle panel show the radial velocities as a function of orbital phase (expressed in days), along with the model (solid line). The bottom panel is a close-up near the mid-transit time. In all cases, the residuals (observed–calculated) are plotted beneath the data.

we simulated RM spectra with the same data format and noise characteristics as the actual data, and determined the Doppler shifts using the same algorithm used on the actual data. The simulations were based on a “template” spectrum representing the emergent spectrum from a small portion of the photosphere. We scaled the template spectrum in flux by ϵ and shifted it in velocity by v_p , representing the spectrum of the occulted portion of the stellar disk. We subtracted this spectrum from a rotationally-broadened version of the template spectrum (broadened to 3 km s^{-1} to mimic the disk-integrated spectrum of HD 189733), and then “measured” the anomalous Doppler shift Δv . This was repeated for a grid of $\{\epsilon, v_p\}$, and a polynomial function was fitted to the resulting surface.

The template spectrum should be similar to that of HD 189733 but without significant rotational broadening. We tried three different choices: two empirical spectra, and one theoretical spectrum. The two empirical spectra were Keck/HIRES spectra ($\text{SNR} \approx 800$, $R \approx 10^5$) of HD 3561 (G3 V, $v \sin i_S = 1.2 \pm 0.5 \text{ km s}^{-1}$) and HD 3765 (K2 V, $0.0 \pm 0.5 \text{ km s}^{-1}$). The former is 200 K hotter than HD 189733, while the latter is more metal-rich. The theoretical spectrum, with a resolution of 250,000, was taken from Coelho et al. (2005) for a non-rotating star with $T_{\text{eff}} = 5000 \text{ K}$, $\log g = 4.5$, and $[\text{Fe}/\text{H}] = 0.0$.

For each choice of the template spectrum, we derived the relation between Δv , ϵ , and v_p , and optimized the model as described below. With one exception, the results did not depend significantly on the choice of template spectrum (in the sense that measurement errors caused much larger uncertainties). The single exception was $v \sin i_S$, for which the results differed as much as 3%. For our final analysis, we used the relation

$$\Delta v = -\epsilon v_p \left[1.252 - 0.351 \left(\frac{v_p}{3 \text{ km s}^{-1}} \right)^2 \right] \quad (1)$$

derived from the empirical templates, but we also included an extra error term of 6% in $v \sin i_S$ as a conservative estimate of the systematic error. In summary, the projected separation of the planet and the star determines the transit depth ϵ and the sub-planet rotation velocity² v_p , and then Eq. (1) is used to calculate the anomalous Doppler shift.

The fitting statistic was

$$\chi^2 = \sum_{j=1}^{86} \left[\frac{v_j(\text{obs}) - v_j(\text{calc})}{\sigma_{v,j}} \right]^2 + \sum_{j=1}^{752} \left[\frac{f_j(\text{obs}) - f_j(\text{calc})}{\sigma_{f,j}} \right]^2 + \left(\frac{\Delta\gamma}{12 \text{ m s}^{-1}} \right)^2 + \left(\frac{M_S/M_\odot - 0.82}{0.03} \right)^2, \quad (2)$$

²The sub-planet velocity is the projected rotation velocity of the portion of the star hidden by the planet, and is calculated assuming no differential rotation, an assumption justified by Gaudi & Winn (2006).

where $f_j(\text{obs})$ is the flux observed at time j , $\sigma_{f,j}$ is the corresponding uncertainty, and $f_j(\text{calc})$ is the calculated value. A similar notation applies to the velocities. The last two terms are *a priori* constraints explained below.

It is important for $\sigma_{f,j}$ and $\sigma_{v,j}$ to include not only measurement errors but also any unmodeled systematic errors. To account for systematic errors in the photometry, we increased the Poisson estimates of the errors by a factor of 1.2, at which point $\chi^2/N_{\text{DOF}} = 1$ when fitting only the fluxes. Determining the appropriate weights for the velocities was more complex. HD 189733 is chromospherically active and should exhibit velocity noise (“photospheric jitter”) with an amplitude of 11 m s^{-1} according to the empirical relations of Wright (2005). However, the time scale of the noise cannot be predicted as easily. Noise from spots or plagues would occur on the time scale of the rotation period (≈ 13 days), while noise from oscillations and flows occurs on shorter time scales.

We took the following approach. First, we fitted only the 16 velocities obtained sporadically prior to 2006 Aug 21, and found the root-mean-squared (RMS) residual to be 12 m s^{-1} , in agreement with the Wright (2005) relations. Therefore, for fitting purposes, we inflated the error bars $\sigma_{v,j}$ of those 16 velocities to 12 m s^{-1} . Second, we fitted only the 44 *out-of-transit* velocities measured on 2006 Aug 21, and found the RMS residual to be 1.5 m s^{-1} . In addition, there were correlations in the residuals on a time scale of ~ 15 minutes (~ 4 data points). The correlations effectively reduce the number of independent data points by 4, or equivalently, they double the error per point. Therefore, for fitting purposes, we inflated the error bars $\sigma_{v,j}$ of all the 2006 Aug 21 velocities to 3 m s^{-1} . Apparently, for HD 189733, most of the velocity noise occurs on a time scale longer than one night.

Our free parameters were the two bodies’ masses and radii (M_S , M_P , R_S and R_P); the orbital inclination (i); the mid-transit time (T_c); the line-of-sight stellar rotation velocity ($v \sin i_S$); the angle between the projected stellar spin axis and orbit normal (λ ; see Ohta et al. 2005 or Gaudi & Winn 2006 for a diagram of the coordinate system); the velocity zero point (γ); a velocity offset specific to the night of 2006 Aug 21 ($\Delta\gamma$); and a long-term velocity gradient $\dot{\gamma}$. The parameter $\Delta\gamma$ is needed because of the photospheric jitter; the first *a priori* constraint in Eq. (2) enforces a reasonable level of noise. The gradient $\dot{\gamma}$ was included to account for the long-period orbit of HD 189733 and its companion star (Bakos et al. 2006a) or possible long-period planets. We fixed the orbital period to be 2.218575 days (Bouchy et al. 2005, Hébrard & Lecavelier Des Etangs 2006). A well-known degeneracy prevents M_S , R_S , and R_P from being determined independently. We broke this degeneracy with the second *a priori* constraint in Eq. (2), which enforces the spectroscopic determination of M_S by Bouchy et al. (2005).

We used a Markov Chain Monte Carlo algorithm to solve for the model parameters and

their uncertainties (see, e.g., Tegmark et al. 2004 or Ford 2005). Our jump function was the addition of a Gaussian random number to each parameter value. We set the perturbation sizes such that $\sim 20\%$ of jumps are executed. We created 10 independent chains, each with 500,000 points, starting from random initial positions, and discarded the first 20% of the points in each chain. The Gelman & Rubin (1992) R statistic was close to unity for each parameter, a sign of good mixing and convergence. We merged the chains and took the median value of each parameter to be our best estimate, and the standard deviation as the 1σ uncertainty. For the special case of $v \sin i_S$, we added an additional error of 6% in quadrature, due to the systematic error noted previously.

4. Results

The results are given in Table 2. Those parameters depending chiefly on the photometry (R_P , R_S , i) are in agreement with the most accurate results reported previously (Bakos et al. 2006b). Likewise, our result for the planetary mass, $M_P = 1.13 \pm 0.03 M_{\text{Jup}}$, agrees with the value $1.15 \pm 0.04 M_{\text{Jup}}$ measured by Bouchy et al. (2005). Our result for the projected rotation velocity is $v \sin i_S = 3.0 \pm 0.2 \text{ km s}^{-1}$. This agrees with the value $3.5 \pm 1.0 \text{ km s}^{-1}$ reported by Bouchy et al. (2005), which was based on the line broadening in their disk-integrated stellar spectrum. It also agrees with the value $3.2 \pm 0.7 \text{ km s}^{-1}$ based on a similar analysis of our own Keck spectra (D. Fischer, private communication). The most interesting result is $\lambda = -1^\circ.4 \pm 1^\circ.1$. The sky projections of the stellar spin axis and the orbit normal are aligned to within a few degrees.

5. Summary and Discussion

We have monitored the apparent Doppler shift of HD 189733 during a transit of its giant planet. By modeling the RM effect, we find that the stellar spin axis and the orbit normal are aligned to within a few degrees.

This is the third exoplanetary system (and the third hot Jupiter) for which it has been possible to measure λ . The first system was HD 209458, for which $\lambda = -4^\circ.4 \pm 1^\circ.4$ (Winn et al. 2005; see also Wittenmyer et al. 2005, who modeled the RM effect but required $\lambda = 0$). The second system was HD 149026 (Wolf et al. 2006), for which $\lambda = 11 \pm 14^\circ$. The small observed values of λ suggest that the most common end-state of the inward migration of a hot Jupiter involves a close alignment.

With only 3 systems, we cannot yet measure the distribution of λ , but we can test the

hypothesis of random orientations (i.e., a uniform distribution in λ). The weighted mean of the measured values of $|\lambda|$ is 2.6° . If we replace the measured values by random numbers drawn from a uniform distribution, the probability that the weighted mean³ will be this small is only 0.04%. Hence we rule out the hypothesis of random orientations with 99.96% confidence.

Winn et al. (2005) argued that tides from the star would not ordinarily cause alignment within the star’s main-sequence lifetime. There are therefore two basic possibilities: either the alignment is primordial and was not disturbed by migration, or there was a different mechanism to damp any initial or induced misalignment. Among the various theories of hot Jupiter migration, some would tend to enhance any initial misalignments, and are thereby constrained by our results. Such scenarios include planet-planet scattering followed by circularization (Rasio & Ford 1996, Weidenschilling & Marzari 1996), Kozai migration (Wu & Murray 2003; Eggenberger et al. 2004), and tidal capture (Gaudi 2003).

The agreement among the three systems studied to date is clear, but should not discourage future measurements. Obviously, a sample of three is only barely sufficient to draw a conclusion. And of course, the discovery of even a single example of a grossly misaligned system would be of great interest.

We thank Debra Fischer for running SME on our spectra, and Scott Gaudi for very helpful discussions. We recognize and acknowledge the very significant cultural role and reverence that the summit of Mauna Kea has always had within the indigenous Hawaiian community. We are most fortunate to have the opportunity to conduct observations from this mountain.

REFERENCES

- Bakos, G. Á., Pál, A., Latham, D. W., Noyes, R. W., & Stefanik, R. P. 2006, *ApJ*, 641, L57
- Bakos, G. Á., et al. 2006, *ApJ*, submitted [astro-ph/0603291]
- Beck, J. G., & Giles, P. 2005, *ApJ*, 621, L153
- Bouchy, F., et al. 2005, *A&A*, 444, L15

³Here we have assumed the uncertainty in λ is independent of λ , a good approximation because all 3 systems have an intermediate impact parameter (Gaudi & Winn 2006).

- Bundy, K. A., & Marcy, G. W. 2000, *PASP*, 112, 1421
- Butler, R. P., Marcy, G. W., Williams, E., McCarthy, C., Dosanji, P., & Vogt, S. S. 1996, *PASP*, 108, 500
- Butler, R. P., Marcy, G. W., Williams, E., Hauser, H., & Shirts, P. 1997, *ApJ*, 474, L115
- Claret 2004, *A&A*, 428, 1001
- Coelho, P., Barbuy, B., Meléndez, J., Schiavon, R. P., & Castilho, B. V. 2005, *A&A*, 443, 735
- Cox, A. N. 2000, *Allen’s astrophysical quantities*, 4th ed. (New York: AIP Press)
- Deming, D., Harrington, J., Seager, S., & Richardson, L. J. 2006, *ApJ*, 644, 560
- Dobbs-Dixon, I., Lin, D. N. C., & Mardling, R. A. 2004, *ApJ*, 610, 464
- Ford, E. B. 2005, *AJ*, 129, 1706
- Gaudi, B. S. 20003 (astro-ph/0307280)
- Gaudi, B. S. & Winn, J. N. 2006, *ApJ*, submitted [astro-ph/0608071]
- Gelman, A. & Rubin, D. B. 1992, *Stat. Sci.*, 7, 457
- Giménez, A. 2006, *ApJ*, 650, 408
- Halbwachs, J. L., Mayor, M., & Udry, S. 2005, *A&A*, 431, 1129
- Hébrard, G., & Lecavelier Des Etangs, A. 2006, *A&A*, 445, 341
- Mandel, K., & Agol, E. 2002, *ApJ*, 580, L171
- Marcy, G., Butler, R. P., Fischer, D., Vogt, S., Wright, J. T., Tinney, C. G., & Jones, H. R. A. 2005, *Progress of Theoretical Physics Supplement*, 158, 24
- Mayor, M., & Queloz, D. 1995, *Nature*, 378, 355
- Ohta, Y., Taruya, A., & Suto, Y. 2005, *ApJ*, 622, 1118
- Papaloizou, J. C. B. & Terquem, C. 2005, *Rept. Prog. Phys.* 69, 119
- Queloz, D., Eggenberger, A., Mayor, M., Perrier, C., Beuzit, J. L., Naef, D., Sivan, J. P., & Udry, S. 2000, *A&A*, 359, L13

- Rasio, F. A., & Ford, E. B. 1996, *Science*, 274, 954
- Rasio, F. A., Tout, C. A., Lubow, S. H., & Livio, M. 1996, *ApJ*, 470, 1187
- Tegmark, M., et al. 2004, *Phys. Rev. D*, 69, 103501
- Thommes, E. W., & Lissauer, J. J. 2005, *Astrophysics of Life*, 41
- Trilling, D. E. 2000, *ApJ*, 537, L61
- Vogt, S. S., et al. 1994, *Proc. SPIE*, 2198, 362
- Weidenschilling, S. J., & Marzari, F. 1996, *Nature*, 384, 619
- Winn, J. N., et al. 2005, *ApJ*, 631, 1215
- Wittenmyer, R. A., et al. 2005, *ApJ*, 632, 1157
- Wolf, A. et al. 2006, *ApJ*, in press
- Wright, J. T. 2005, *PASP*, 117, 657

Table 1. Radial Velocities of HD 189733

JD	Radial Velocity [m s ⁻¹]	Measurement Uncertainty [m s ⁻¹]
2452832.881794	−13.964	1.542
2452898.800937	186.717	1.480
2453180.918877	153.226	1.609
2453240.898507	121.542	1.139
2453303.750382	−202.928	1.244
2453303.753576	−203.187	1.139
2453551.963519	−126.301	1.205
2453693.688738	15.243	1.228
2453694.690856	−84.160	1.180
2453695.688148	125.535	1.259
2453696.700914	−206.994	1.302
2453723.712604	−2.524	1.217
2453926.035150	159.489	1.193
2453926.887766	−141.263	1.107
2453927.929745	53.300	1.157
2453934.845208	179.802	1.224
2453968.722037	57.606	0.787
2453968.724225	57.726	0.802
2453968.726447	56.423	0.832
2453968.728750	56.045	0.755
2453968.731227	54.711	0.848
2453968.733611	52.911	0.798
2453968.736007	50.628	0.789
2453968.757928	42.772	0.726
2453968.760266	38.559	0.760
2453968.762639	36.305	0.746
2453968.765023	37.873	0.741
2453968.767419	34.160	0.818
2453968.769826	33.982	0.768
2453968.772280	32.973	0.657
2453968.774757	30.196	0.740

Table 1—Continued

JD	Radial Velocity [m s ⁻¹]	Measurement Uncertainty [m s ⁻¹]
2453968.777245	29.968	0.662
2453968.779688	28.832	0.651
2453968.782095	28.517	0.764
2453968.784525	27.562	0.772
2453968.786979	26.713	0.682
2453968.789433	25.029	0.682
2453968.791910	24.544	0.749
2453968.794433	20.275	0.661
2453968.796944	21.667	0.855
2453968.799456	28.013	0.803
2453968.802049	31.972	0.780
2453968.804745	39.982	0.797
2453968.807373	45.933	0.816
2453968.810000	47.080	0.857
2453968.812650	49.130	0.870
2453968.815289	45.655	0.982
2453968.818021	42.260	0.994
2453968.820718	34.659	0.965
2453968.823391	27.992	0.987
2453968.826134	18.132	0.905
2453968.828912	7.218	0.858
2453968.831806	−0.572	1.007
2453968.834687	−5.327	0.846
2453968.839641	−24.613	0.751
2453968.842905	−34.630	0.885
2453968.845845	−41.573	0.935
2453968.848877	−45.183	0.842
2453968.851991	−47.586	0.972
2453968.855220	−47.746	1.009
2453968.858356	−44.215	0.928
2453968.861354	−37.956	0.820

Table 1—Continued

JD	Radial Velocity [m s ⁻¹]	Measurement Uncertainty [m s ⁻¹]
2453968.864352	−30.035	0.943
2453968.867361	−27.041	0.890
2453968.870301	−25.215	0.985
2453968.873183	−24.080	0.961
2453968.876076	−22.205	0.892
2453968.878912	−27.297	0.866
2453968.881782	−28.557	0.907
2453968.884583	−29.194	0.822
2453968.887569	−33.236	0.807
2453968.890498	−33.070	0.638
2453968.893403	−31.439	0.847
2453968.896331	−36.218	0.712
2453968.899271	−39.051	0.757
2453968.902118	−41.663	0.900
2453968.904931	−42.919	0.748
2453968.907639	−45.150	0.876
2453968.910278	−42.636	0.956
2453968.912940	−43.977	0.818
2453968.915637	−47.332	0.828
2453968.933565	−58.550	0.715
2453968.955347	−69.951	0.771
2453968.977743	−79.481	0.754
2453969.002674	−95.622	0.750
2453969.032870	−112.396	0.898

Note. — Column 1 gives the Julian Date at the time of the photon-weighted mid-exposure. Column 3 gives the measurement uncertainties, which do *not* include the estimated photospheric jitter (see § 3).

Table 2. System Parameters of HD 189733

Parameter	Value	Uncertainty
M_S/M_\odot	0.82	0.03
M_P/M_{Jup}	1.13	0.03
R_S/R_\odot	0.73	0.02
R_P/R_{Jup}	1.10	0.03
i [deg]	86.1	0.2
T_c [HJD]	2453937.7759	0.0001
$v \sin i_S$ [km s ⁻¹]	2.97	0.22
λ [deg]	-1.4	1.1
γ [m s ⁻¹]	5.0	10.1
$\Delta\gamma$ [m s ⁻¹]	-15.0	4.8
$\dot{\gamma}$ [m s ⁻¹ yr ⁻¹]	-1.9	3.3